Traveling waves in a fluid layer subjected to a horizontal temperature gradient

F. Daviaud and J. M. Vince
Service de Physique de l'Etat Condensé, Commissariat à l'Energie Atomique, Centre d'Etudes de Saclay, F-91191 Gif-sur-Yvette Cedex, France
(Received 2 August 1993)

We report experimental observations of traveling waves in a pure fluid with a free surface situated in a long container submitted to a horizontal temperature gradient perpendicular to its large extension. Above a critical value of the gradient and depending on the height of liquid h, a source of propagating waves is created in the container for small values of h, while stationary patterns arise for larger values of h. The spatiotemporal properties of the waves are studied and compared to available theoretical predictions.

PACS number(s): 47.20.−k, 47.27.−i, 47.35.+i

I. INTRODUCTION

While the nature of turbulence in fluids is still an open question, the evolution towards turbulent states has received much attention in the last decade and important results have been obtained in weakly confined systems. Studies of one- or two-dimensional (1D or 2D) systems in numerical models and experiments have shown that a periodic stationary or propagating state may destabilize when a control parameter is varied and become turbulent via different scenarios. A transition to turbulence via spatiotemporal intermittency has been observed in models of phase equations [1] and coupled-map lattices [2] as well as in 1D Rayleigh-Bénard convector [3], in the printer's instability [4] or in capillary ripples [5]. The dynamics of propagating patterns has been widely studied in Ginzburg-Landau equations [6] or in convection in binary fluid mixtures [7]. The destabilization of these patterns leads to spatiotemporal chaos.

The existence of propagating waves has also been predicted in convection in pure fluids with a free surface, when a horizontal temperature gradient is applied [8–10]. These waves are not observed in small containers [11] but they are present in float-zone crystal growth, even in the absence of gravity, and play an important role in the transport of impurities. These last experiments are generally performed in cylindrical geometries and on low-Prandtl-number liquids [12], configurations in which quantitative measurements are difficult to obtain. Very few experiments have been performed to characterize these waves and to study their destabilization. 1D propagative patterns have been observed in an experiment involving a hot wire below the free surface of a liquid [13] but the physical mechanisms responsible for this instability remain unknown. The existence of hydrothermal waves has also been recently reported in Bénard-Marangoni convection in a cylindrical container with a hot source in the central part [14]. In this case, the waves appear as concentric rolls traveling radially from the center.

In this article, we report experimental results concerning different dynamical regimes, including waves traveling perpendicularly to the temperature gradient, obtained in a very simple configuration. A pure fluid with a free surface is situated in a long and narrow container and is submitted to a horizontal temperature gradient perpendicular to its large extension. Our system thus appears to be a good tool to study both the mechanisms which drive this instability and the dynamics of nonlinear 1D traveling waves.

II. EXPERIMENTAL SETUP

The apparatus consists of a rectangular container 20-cm long and 1-cm wide (see Fig 1). The long vertical walls are made of copper and can be thermally regulated by circulating water. The container is closed by two narrow plexiglass walls. The lower boundary consists of a glass plate for observations while a plexiglass plate is inserted a few millimeters above the surface of the fluid to avoid evaporation. The container is filled with silicone oil (viscosity $\nu=0.0065$ Stokes) of Prandtl number $P=10$ to a height h that is measured with a precision of 0.05 mm. The horizontal temperature gradient ΔT is imposed by the two copper walls and is measured using thermocouples. This gradient is regulated with a stability of 10^{-2} K.

The patterns are visualized by shadowgraphic imaging. A parallel vertical light beam crosses the container from top to bottom and forms a horizontal picture on a screen, due to surface deformations at the oil-air interface and to temperature gradients in the fluid (see Fig. 2). The spa-

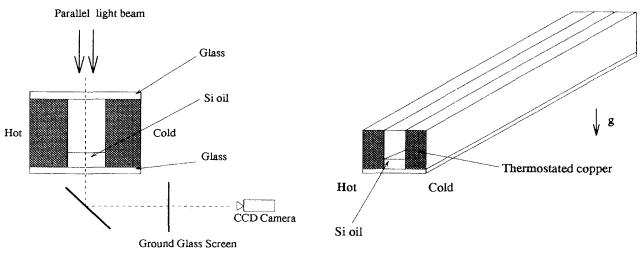

FIG. 1. Schematic drawing of the experimental apparatus.

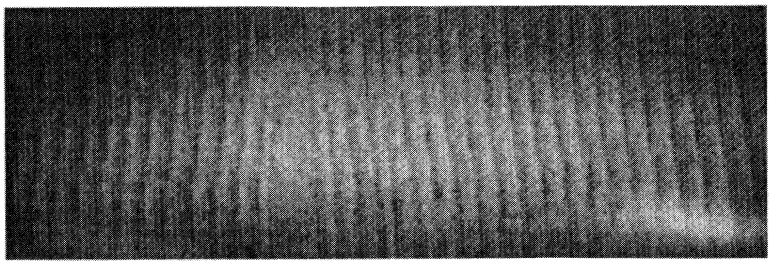

FIG. 2. Shadowgraphic image of a traveling wave pattern in a horizontal plane for $h=1$ mm and $\Delta t=5.5$ K. The top (respectively the bottom) of the picture corresponds to the hot (respectively the cold) plate.

tiotemporal evolution of the structures is recorded using a video camera and the images are digitized along a line of 512 pixels perpendicular to the gradient. This method is described in detail elsewhere [15].

III. EXPERIMENTAL RESULTS

The two parameters which control our experimental system are h, the height of silicone oil in the cell, and ΔT, the horizontal temperature difference between the two walls. We have observed that, for each h value, when ΔT is increased from zero to a threshold value ΔT_c, a longitudinal (parallel to the gradient) pattern appears. Depending on the height of liquid, two regimes occur. When $\Delta T \geq \Delta T_c$, for small h values (from 0 to 2.8 mm), the system exhibits longitudinal waves propagating perpendicularly to the gradient (see Fig. 2) while, for larger h values (from 2.8 to 10 mm), stationary "rolls" with axes parallel to the gradient are observed. Figure 3 shows the dependence of ΔT_c, on h for these two kinds of structures. The height, $h=2.8$ mm, at which the two domains meet corresponds to a unit ratio between the Marangoni and the Rayleigh number,

$$W=\mathrm{Ma}/\mathrm{Ra}\simeq 1$$

with

$$\mathrm{Ma}=-(\partial\sigma/\partial T)\Delta T h/\rho_0\kappa\nu \text{ and } \mathrm{Ra}=g\alpha\Delta T h^3/\kappa\nu ,$$

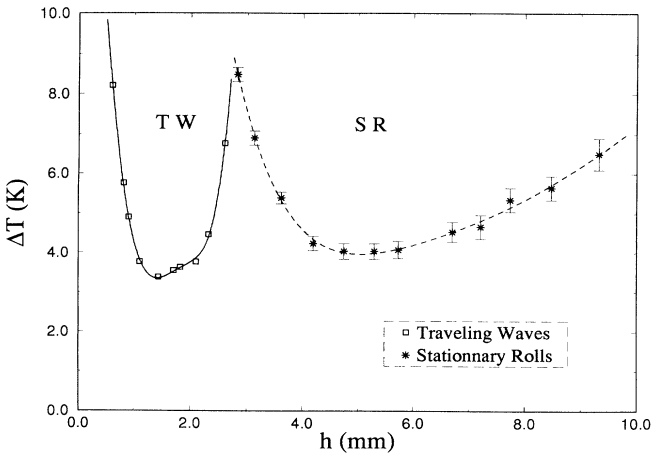

FIG. 3. Critical temperature difference ΔT_c vs the height of liquid h.

where g is the gravitational acceleration, α the thermal expansion coefficient, κ is the thermal diffusivity, ρ_0 is the density of the fluid, ν is the kinematic viscosity, and σ is the surface tension. The traveling wave domain corresponds to $W>1$, where surface tension effects are dominant, while in the stationary roll domain ($W<1$) buoyancy is dominant.

In the regime of propagating waves, when ΔT is increased above ΔT_c, a source of waves is created in the container while two sinks are generally situated at the edges of the container (cf. Fig. 2). By calculating the amplitude of the waves by complex demodulation techniques, we see that this source corresponds to a region of reduced amplitude (a "hole," cf. Figs. 4 and 5). Moreover, its dimension depends on $\epsilon=(\Delta T-\Delta T_c)/\Delta T_c$. The size of the source is very large near the threshold and decreases in length as ϵ is increased. If ΔT is increased very quickly above ΔT_c, several defects are created, and pairs of sources and sinks vanish until only one source and one or two sinks remain. The waves are not exactly perpendicular to the large side of the container but exhibit an angle $\psi\simeq 80°$. This angle does not seem to depend on ΔT or on h.

We have constructed space-time diagrams to study the dynamics of the waves (see Fig. 4). With such diagrams, the wave length and the period of these waves can easily be measured. Spatial and temporal Fourier spectra reveal that the waves have a unique wavelength and frequency at threshold. For h between 0 and 2.5 mm, the period at threshold τ_c increases with h [cf. Fig. 6(a)]. In the same range of h, the λ_c/h variation versus h is nonmonotonic, with a maximum for $h=1.4$ mm [cf. Fig. 6(b)].

We have also performed some measurements for ΔT larger than ΔT_c at different h. The curves giving the period τ and the phase velocity v_φ versus ϵ are displayed in Figs. 7(a) and 7(b), respectively. The figures show that τ decreases and v_φ increases when ϵ is increased. For small h, τ and v_φ are clearly different from those obtained for the middle range of h, showing the sensitivity to surface tension effects which are more important for small h. Finally, when ϵ is further increased, the system of traveling waves exhibits phase instabilities leading to space-time dislocations (cf. Fig. 8).

Stationary rolls are strictly perpendicular to the large side of the cell, unlike traveling waves. The wavelength of these rolls appears to be proportional to the height of liquid h. When ϵ is increased, the rolls begin to oscillate in an optical mode. For larger ϵ, the pattern destabilizes

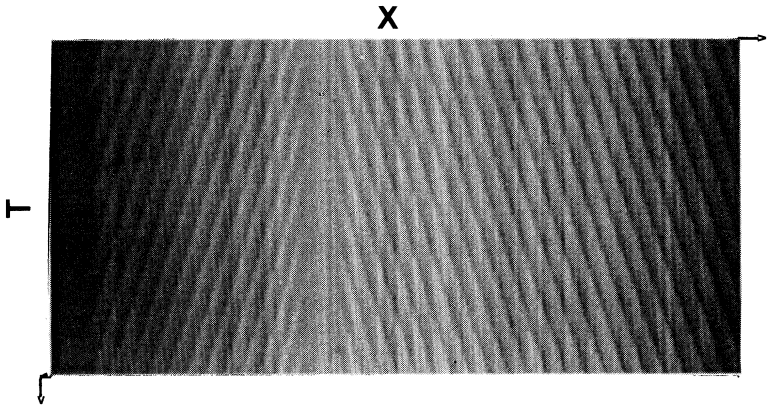

FIG. 4. Spatiotemporal evolution showing a left- and a right-going wave emitted from a source and corresponding to the pattern shown in Fig. 2. The total acquisition time is 25 sec and the spatial extension is 20 cm.

and gives place to spatiotemporal chaos. These dynamical regimes are reminiscent of Rayleigh-Bernard convection in narrow gap geometries [3,15].

IV. DISCUSSION

Our observations raise several interesting hydrodynamic and phenomenological issues. First, thermocapillarity appears to be the main physical mechanism driving the instability for small h, while buoyancy is dominant for large h. A temperature gradient imposed on a thin fluid layer with a free surface produces a corresponding gradient in surface tension and hence a bulk fluid motion [9]. For our fluid, the surface tension is a decreasing function of temperature ($\partial\sigma/\partial T < 0$) so that there is surface flow from the hot towards the cold side of the container. Although we have not yet recorded velocity profiles, by seeding the flow with particles and illuminating it with a laser sheet, we have seen that the horizontal velocity profile includes a shear flow near the surface and return flow at the bottom, the convection being monocellular (cf. [11]).

Smith and Davis have shown that this dynamic state can destabilize into two thermoconvective instabilities: stationary longitudinal rolls and traveling hydrothermal waves [8]. They consider the estabilization of two basic flow profiles: the linear flow state (LFS) and the return flow state (RFS). They calculate the critical conditions Ma_c versus P. In the LFS, when $P > 1.6$, there is station-

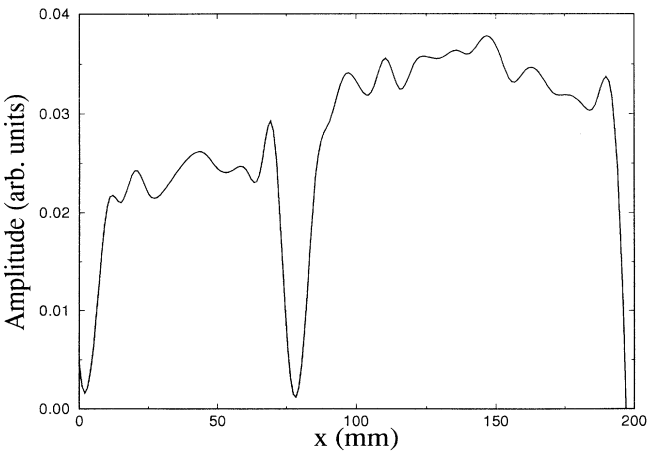

FIG. 5. Amplitude of the waves corresponding to Fig. 4 as a function of space x.

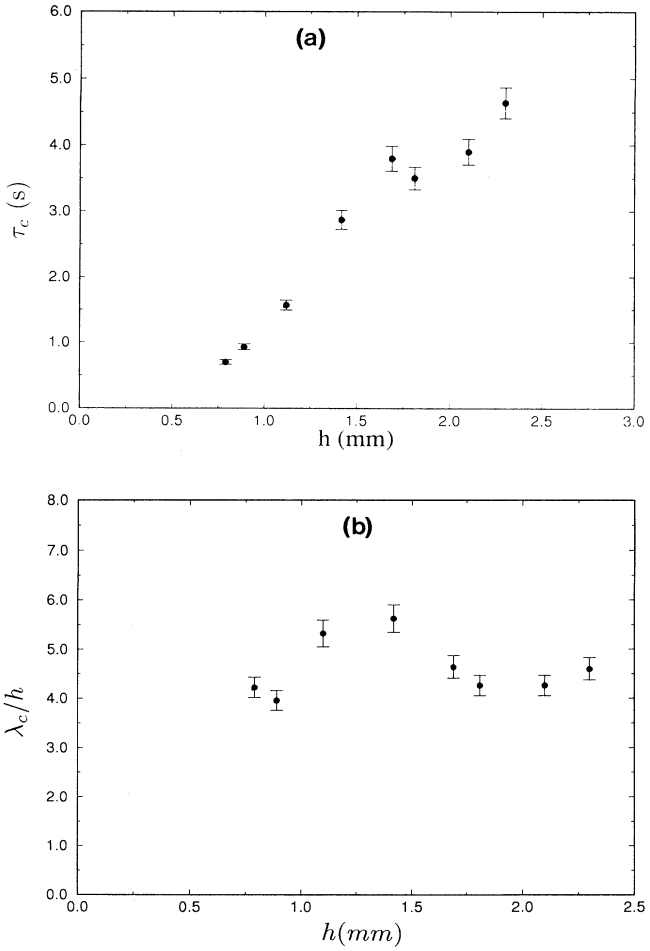

FIG. 6. Evolution of the period τ_c (a) and of the wavelength λ_c/h (b) with the height of liquid h.

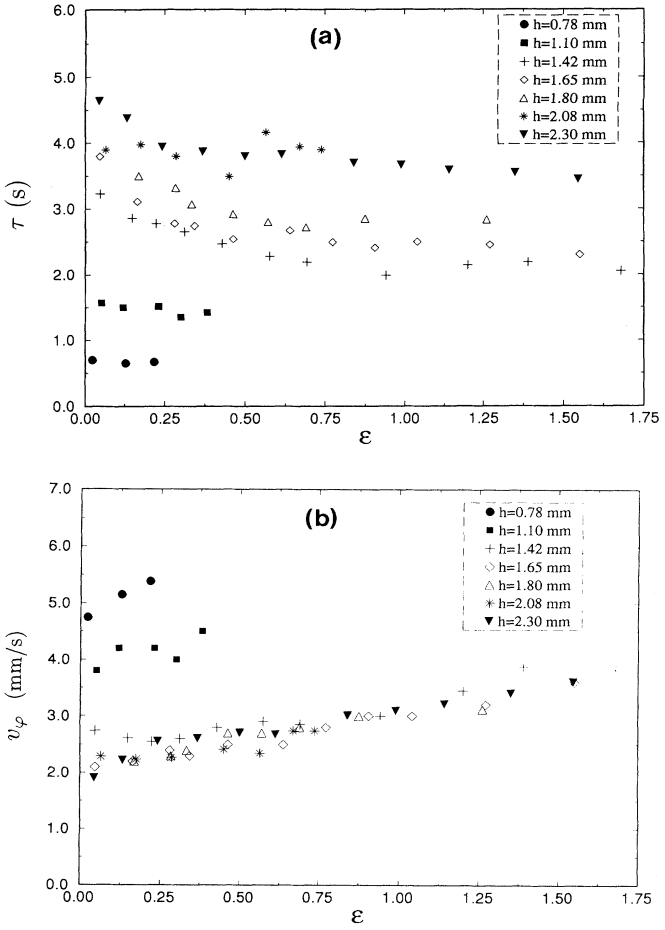

FIG. 7. Evolution of the period τ (a) and of the velocity v_φ (b) of the waves with the reduced temperature difference ϵ.

ary convection in the form of rolls parallel to the gradient. 2D waves traveling in the direction of the gradient are observed when $0.6 < P < 1.6$. When $P < 0.6$ there are oblique hydrothermal waves that are traveling perpendicularly to the gradient ($\psi \simeq 90°$). In the RFS, the preferred mode is an oblique hydrothermal wave, with an angle of propagation ψ that that decreases with P increasing: for $P = 10$, $\psi \simeq 20°$. The physical mechanisms describing these instabilities are described in Refs. [9] and [16], but the main difference between hydrothermal instability at small P and at large P is the following. Instability arises for small P (respectively for large P) from a transfer of energy from the imposed horizontal temperature gradient (respectively the vertical flow induced temperature field) to the disturbances through a horizontal (respectively vertical) convection mechanism.

Our experimental results show the same instabilities as those predicted by Smith and Davis: stationary rolls parallel to the gradient and waves propagating perpendicularly to the gradient. However, some differences remain. First, our basic flow is closer to their RFS, in which no stationary state is observed. Moreover, our results have been obtained with a fluid of $P = 10$, for which oblique traveling waves are not predicted in the LFS and are predicted in the RFS, but with an angle of 20° in contradiction to the experiment. For $h = 0.8$ mm, the experimental results give a critical Marangoni number $\mathrm{Ma}_c \simeq 12000$, a critical wave number $\sigma_c \simeq 1.5$, and a reduced phase velocity $v_c \simeq 0.06$. These values can be compared to those obtained in the RFS: $\mathrm{Ma}_c^{\mathrm{RFS}} \simeq 300$, $\sigma_c^{\mathrm{RFS}} \simeq 2.6$, and $v_c^{\mathrm{RFS}} \simeq 0.06$. The differences between experiment and theory are even larger for larger h.

These differences could be explained by the absence of gravity in the model of Smith and Davis. More recently, the stability of convective motion in a differentially heated cavity has been studied, in the presence of gravity, for small-Prandtl-number liquids [17] and in the limit of large ΔT [18]. A linear stability analysis has also been performed in the general case and shows similar instabilities [19]. However, certainly due to different boundary conditions, our experimental observations differ from the results displayed in Ref. [19]. A more realistic model including both surface tension and gravity together with appropriate boundary conditions is currently being studied and the first results are promising [20].

The instabilities observed in our experiment are also different from the results obtained by Ezersky *et al.* in a cylindrical geometry [14]. In their case, the stationary rolls are concentric and thus perpendicular to gradient, and the waves propagate radially from the center (parallel to the gradient). These differences could be due to the geometry or to the boundary conditions.

Phenomenologically, our configuration is a good sys-

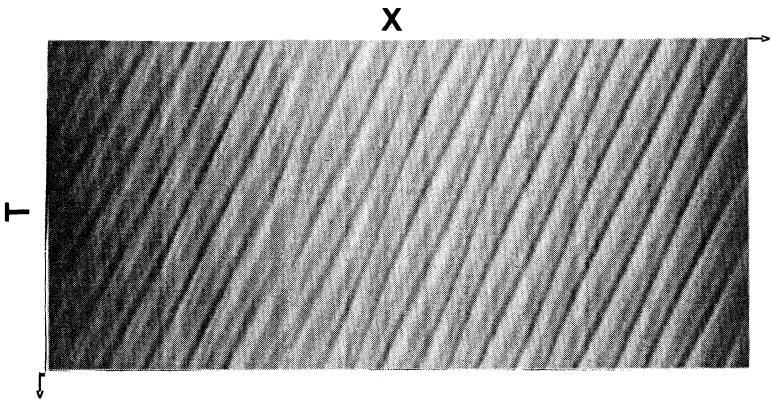

FIG. 8. Spatiotemporal evolution showing phase instabilities for $h = 1.5$ mm and $\Delta T = 10$ K.

tem for exploring nonlinear 1D traveling waves and their destabilization. The spatiotemporal properties of the waves can be studied in the frame of two coupled amplitude equations that can be derived from a physical model [20]. They have general properties that do not depend on the exact experimental system.

By using a nonlinear multiple-scale analysis, Smith has derived these equations in the absence of gravity [10]. His analysis expects the system to develop into a pure-wave state consisting of either the right or the left linear wave, except for small P where a combination of both of the waves should develop. In our experiment, the presence of a source stabilizes the right- and left-going waves with a definite wavelength. Near threshold, the width of the source increases with decreasing ϵ, as observed in the hot wire experiment [13] and in recent numerical simulations [21]. When ϵ is increased, the phase instabilities which are observed (cf. Fig. 8) could be related to an Eckhaus or a Benjamin-Feir Instability [10].

In conclusion, our experiment shows the presence of stationary rolls parallel to the imposed thermal gradient and of hydrothermal waves propagating perpendicularly to the gradient. These instabilities are qualitatively similar to those described in theoretical models but many contradictions and differences persist and suggest new theoretical work. We are currently performing experiments using an annular configuration with a radial temperature gradient.

ACKNOWLEDGMENTS

We wish to thank M. Dubois, J. Lega, and C. Normand for stimulating discussions and M. Labouise, P. Hede, and B. Ozenda for their technical assistance.

[1] H. Chaté and P. Manneville, Phys. Rev. Lett. **58**, 112 (1987).
[2] K. Kaneko, Prog. Theor. Phys. **74**, 1033 (1985); H. Chanté and P. Manneville, Physica D **32**, 409 (1988).
[3] S. Ciliberto and P. Bigazzi, Phys. Rev. Lett. **60**, 286 (1988); F. Daviaud, M. Dubois, and P. Bergé, Europhys. Lett. **9**, 441 (1989).
[4] M. Rabaud, S. Michalland, and Y. Couder, Phys. Rev. Lett. **64**, 184 (1990).
[5] N. B. Tufillaro, R. Ramshankar, and J. P. Gollub, Phys. Rev. Lett. **62**, 422 (1989).
[6] P. Coullet and J. Lega, Europhys. Lett. **7**, 511 (1988).
[7] See, e.g., P. Kolodner, D. Bensimon, and C. M. Surko, Phys. Rev. Lett. **60**, 1723 (1988).
[8] M. K. Smith and S. H. David, J. Fluid Mech. **132**, 119 (1983).
[9] S. H. Davis, Annu. Rev. Fluid Mech. **19**, 403 (1987).
[10] M. K. Smith, J. Fluid Mech. **194**, 391 (1988).
[11] See, e.g., D. Villers and J. K. Platten, J. Fluid Mech. **234**, 487 (1992).
[12] F. Preissier, D. Schwabe, and A. Scharmann, J. Fluid Mech. **126**, 545 (1983); J. J. Xu and S. H. Davis, Phys. Fluids **27**, 1102 (1992).
[13] J. M. Vince and M. Dubois, Europhys. Lett. **20**, 505 (1992).
[14] A. B. Ezersky, A. Garcimartin, J. Burguete, H. L. Mancini, and C. Perez-Garcia, Phys. Rev. E **48**, 1126 (1993).
[15] F. Daviaud, M. Bonetti, and M. Dubois, Phys. Rev. A **42**, 3388 (1990).
[16] M. K. Smith, Phys. Fluids **29**, 3182 (1986).
[17] P. Laure and B. Roux, J. Cryst. Growth **97**, 226 (1989).
[18] B. M. Carpenter and G. M. Homsy, J. Fluid Mech. **207**, 121 (1989).
[19] G. Z. Gershuni, P. Laure, V. M. Myznikov, B. Roux, E. M. Zhukhovitsky, Microgravity Quarterly **2**, 141 (1992).
[20] C. Normand and J. Lega (private communication).
[21] F. Plazza and J. M. Vince (private communication).

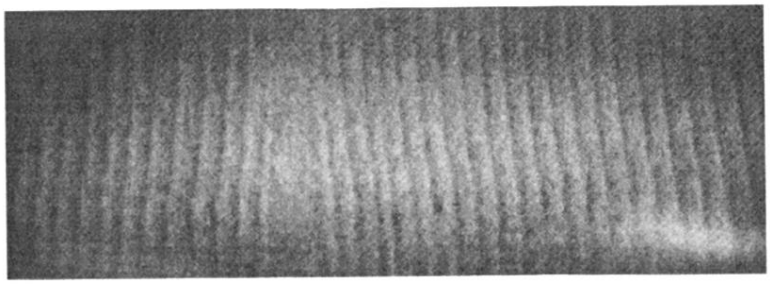

FIG. 2. Shadowgraphic image of a traveling wave pattern in a horizontal plane for $h = 1$ mm and $\Delta t = 5.5$ K. The top (respectively the bottom) of the picture corresponds to the hot (respectively the cold) plate.

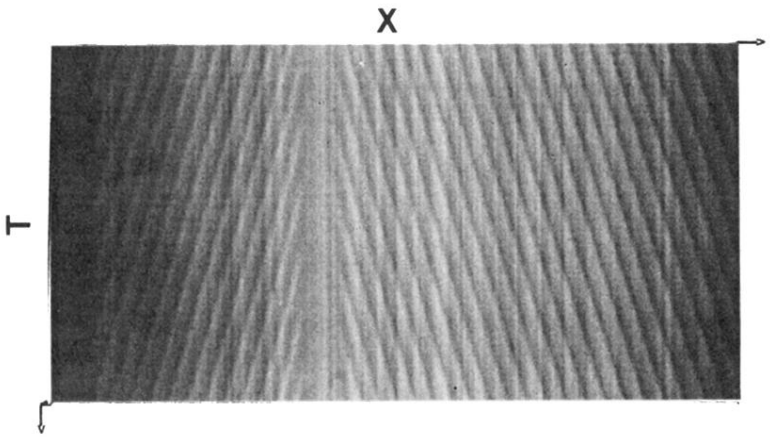

FIG. 4. Spatiotemporal evolution showing a left- and a right-going wave emitted from a source and corresponding to the pattern shown in Fig. 2. The total acquisition time is 25 sec and the spatial extension is 20 cm.

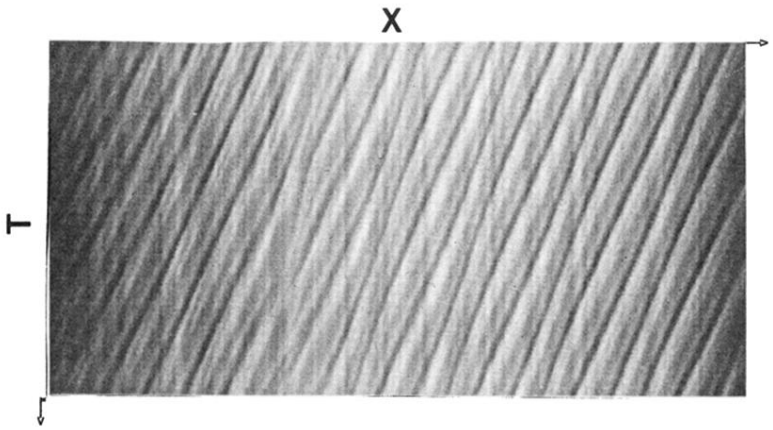

FIG. 8. Spatiotemporal evolution showing phase instabilities for $h = 1.5$ mm and $\Delta T = 10$ K.